KSME International Journal, Vol. 17 No. 10, pp. 1431~1442, 2003

The Position/Orientation Determination of a Mobile-Task Robot Using an Active Calibration Scheme

Tae-Seok Jin*, Jang-Myung Lee

Department of Electronics Engineering, Pusan National University, Pusan 609-735, Korea

A new method of estimating the pose of a mobile-task robot is developed based upon an active calibration scheme. The utility of a mobile-task robot is widely recognized, which is formed by the serial connection of a mobile robot and a task robot. To be an efficient and precise mobile-task robot, the control uncertainties in the mobile robot should be resolved. Unless the mobile robot provides an accurate and stable base, the task robot cannot perform various tasks. For the control of the mobile robot, an absolute position sensor is necessary. However, on account of rolling and slippage of wheels on the ground, there does not exist any reliable position sensor for the mobile robot. This paper proposes an active calibration scheme to estimate the pose of a mobile robot that carries a task robot on the top. The active calibration scheme is to estimate a pose of the mobile robot using the relative position/orientation to a known object whose location, size, and shape are known a priori. For this calibration, a camera is attached on the top of the task robot to capture the images of the objects. These images are used to estimate the pose of the camera itself with respect to the known objects. Through the homogeneous transformation, the absolute position/orientation of the camera is calculated and propagated to get the pose of a mobile robot. Two types of objects are used here as samples of work-pieces : a polygonal and a cylindrical object. With these two samples, the proposed active calibration scheme is verified experimentally.

Key Words : Active Calibration, Mobile Manipulator, Mobile-Task Robot, Camera, Line Correspondence, Conic Correspondence

1. Introduction

There are two major difficulties in the precise control of the mobile robot. One difficulty lies in the dynamic modeling of the mobile robot as other complex structures. The other difficulty lies in the uncertainties of the boundary in between the wheels of the mobile robot and the ground. The friction is nonlinear and time-varying, which we can not either estimate or model exactly. Recently, there are several researches on the accurate control of the mobile robot with the recognition of the environment using the laser, ultrasonic and vision sensors intelligently (Borenstein, 1995 ; Tsai, 1987 ; Lui et al., 1990 ; Luong and Faugeras, 1997 ; Pissard-Gibollet and Rives, 1995).

In this paper, we proposed a method of measuring the position/orientation of the task robot base, that is, the pose of the mobile robot using the images of known objects captured by a camera attached at the end of the task robot (Zhuang and Roth, 1996 ; Han and Lee, 1997 ; Horaud et al., 1997).

Active camera scheme is a recent development (Jang and Han, 1997 ; Crowley and Bobet, 1993) for which the calibration patterns are not necessary. In the active calibration schemes, the feature points on the objects whose locations are given a priori, are utilized to calculate the pose of the

* Corresponding Author,
E-mail : jmlee@pusan.ac.kr
TEL : +82-51-510-2378; **FAX** : +82-51-515-5190
Department of Electronics Engineering, Pusan National University, Pusan 609-735, Korea. (Manuscript **Received** August 12, 2002; **Revised** June 30, 2003)

camera (Du and Brady, 1993; Crowley and Bobet, 1993; Longuet-Higgins, 1981). In this research, the active calibration scheme is properly applied for the pose determination of the mobile robot that does not have any absolute position information. This enables the visual servoing tasks by allowing explicit control of the mobile robot in closed loop with regards to their assembly parts (Jang and Han, 1997).

During the calibration process, the sensitivity and robustness need to be considered (Heyden and Astrom, 1997; Yi et al., 1999). Also some coordinates of a set of lines and ellipsoids may cause numerical instability in obtaining the pose of the camera *w.r.t.* the object (Longuet-Higgins, 1981). In our approach, the task robot is able to carry the camera to a specific position and orientation as desired, the problems can be avoided dynamically. Also this scheme is free from the shape of the objects that the robot is going to handle with. In this paper, we are focusing on the methodology of utilizing the calibration scheme for the localization of the mobile robot instead of searching the numerical problems. In the conventional approaches (Sturm and Maybank, 1999; Zhuang et al., 1991) where calibrations of the camera and the robot are performed in a sequential manner, the errors are propagated and aggregated in the position/orientation determination. However in this approach, the active calibration scheme identifies the camera and robot parameters simultaneously, which suppresses the error propagation.

2. Active Calibration Method of a Mobile/Task Robot

2.1 Perspective model of a camera

A perspective model of a camera represents the relationship between the two dimensional object location on a image plane and the actual object location in a three dimensional space. Figure 1 represents a perspective model of a camera. Here, the coordinates, {W}, is a world frame in the 3-D space, the coordinates, {C}, is a camera frame whose origin is assigned at the center of the lens of the camera. The coordinate, {F}, represents the coordinates in the computer memory frame. The basic axes X_f and Y_f define the coordinate system. Note that Z_c axis is coincident with the optical axis of the camera.

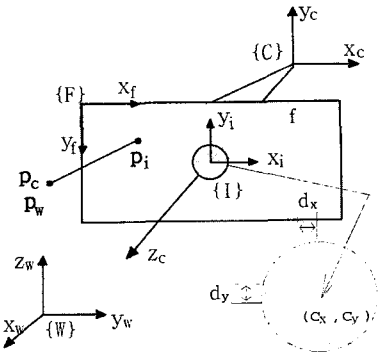

Fig. 1 Perspective model of camera

A point in the space can be represented as a vector, $p_w=(x_w, y_w, z_w)$ *w.r.t.* the reference frame, and it can be also represented as $p_c=(x_c, y_c, z_c)$ *w.r.t.* the camera frame. The coordinates, {I}, represents the image frame of the camera, which is assigned to the image plane of the camera. The effective focal length of the camera, f, represents the distance between the image plane and the origin of camera frame, {C}.

The vector, $p_i=(x_i, y_i)$, on the image plane represents a feature point on the fixed object. The p_w *w.r.t.* the world frame corresponds to the vector, p_c, *w.r.t.* the camera frame. The parameters, dx and dy, represent the size of a pixel along the x axis and y axis respectively, and they can be obtained by using the number of pixels and the image plane of the camera. These parameters are used in transforming the image coordinates to the memory frame. The coordinate, (c_x, c_y) represents the center coordinates of the image in the image frame. It is reported that the value of (c_x, c_y) can be changed within 10 pixels without affecting the measurement accuracy of the three dimensional object (Lui et al., 1990).

In this paper, we assumed that the center of the image frame is located at the center of the image frame. Using the camera perspective model and the transformation of the object location from the world frame to the image frame, basic equations and parameters required for the measurement of

the camera pose can be obtained.

2.2 Camera parameters

The camera parameters to be estimated can be classified into two categories: internal and external parameters. The specification related parameters of the camera and lens, for examples, the focal distance, f, and the image scale factor S, are internal parameters; the rotation matrix, R, and the translational vector, T representing the pose of the moving camera are external parameters. By the coordinates transformation between the robot and camera frames, the positioning vector, p_c, represented in terms of the camera frame can be represented as p_w in terms of the world frame.

$$p_w = Rp_c + T \tag{1}$$

where $R_{3\times3}$ and $T_{3\times1}$ represents a rotation matrix and a translation vector from the world frame to the camera frame, respectively. A positioning vector for a feature point on the three dimensional object in terms of the camera frame, $p_c=(x_c, y_c, z_c)$ is mapped to a point $p_i=(x_i, y_i)$ on the two dimensional image frame using the camera perspective model (Tsai, 1987), and it can be described as follows:

$$x_i = f\frac{x_c}{z_c} \tag{2}$$

$$y_i = f\frac{y_c}{z_c} \tag{3}$$

where f represents the effective focal distance. The image coordinates are obtained by the linear pin-hole model, and the distortion effects of the lens are not considered in this formula.

Since the scale values along x axis and y axis are different in the image frame, a point on the image frame, (x_i, y_i) corresponds to a location in the image frame, (x_f, y_f) according to the following relations:

$$x_i = S_x^{-1}\bar{x}_i \tag{4}$$

$$y_i = S_y^{-1}\bar{y}_i \tag{5}$$

where $\bar{x}_i = d_x(x_f - c_x)$, $\bar{y}_i = d_y(y_f - c_y)$, and S_x and S_y represents the camera scale factor along the x axis and y axis, respectively. Plugging the location value (x_f, y_f) which is obtained through the image processing into (4) and (5), we can represent the feature point on the image frame. Setting the number of y directional scanning lines and the row numbers of pixels to the same, the y axis scale factor becomes unity, that is, $S_y=1$ and S can stand for S_x.

3. Robot/Vision System

A task robot that has 5 links and a gripper, and a mobile robot that has 3 d.o.f are serially connected for this research (Kang et al., 2000). Figure 2 shows the coordinates assigned to this overall system.

The coordinates transformation relationship among the frames of the mobile robot supporting a task robot is shown in Figure 3. { W } is a world frame for the system, { O } is assigned to the fixed object located at a known position, { C } is the

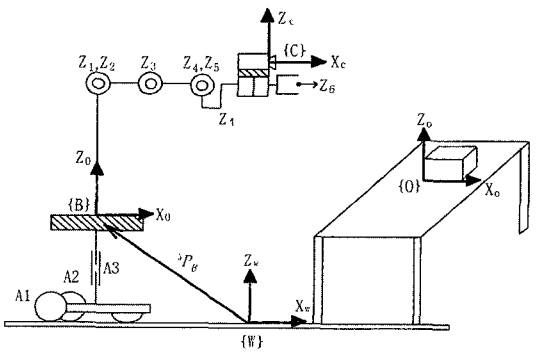

Fig. 2 Link coordinates of mobile robot supporting a task robot

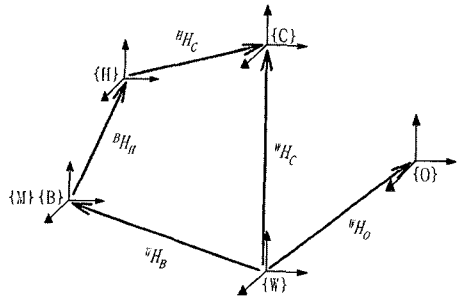

Fig. 3 Coordinates transformation of robot/vision system

camera frame, { H } is the hand frame where the camera is attached, { B } is the base frame of task robot, and { M } is assigned to the top plate of mobile robot. For mathematical conveniences, the frame { B } and { M } are assigned at the same point.

The goal of calibration is measuring the relative position/orientation of the mobile robot with respect to the world frame accurately through the visual information processing of the known object.

For this goal, the calibration task can be decomposed into two steps. The first step is measuring the relative pose of the camera, ${}^{W}H_C$, using the images of the fixed object. The second step is obtaining the homogeneous transformation of the mobile robot *w.r.t.* the world frame, ${}^{W}H_B$, using ${}^{W}H_C$, ${}^{B}H_C$, and ${}^{H}H_C$. This process can be represented by the following equations.

$$ {}^{W}H_B = {}^{W}H_C \cdot {}^{B}H_C^{-1} \tag{6} $$

$$ {}^{B}H_C = {}^{B}H_H \cdot {}^{H}H_C \tag{7} $$

Notice that the structure of the task robot is generally assumed to be light and small. Therefore, ${}^{B}H_C$, can be obtained accurately through the kinematics of the task robot as shown in (7). In the following section, the process of obtaining ${}^{W}H_C$ will be described in detail. As it is shown in Figure 3, ${}^{W}H_C$ is obtained from the images of the fixed object, assuming the location of the object *w.r.t.* the world frame is known a priori. This can be represented as following equation :

$$ {}^{W}H_C^{-1} = {}^{C}H_O \cdot {}^{W}H_O^{-1} \tag{8} $$

where ${}^{O}H_C$ is obtained through the active calibration scheme. For the simplicity, { W } and { O } are assigned to the same location for the later sections.

Note that most of the assembly parts are composed of either line segments or circular segments. Therefore, the active calibration scheme is proposed for each of two cases : 1. An object is composed of only line segments, and 2. An object has both circular segments and line segments.

4. Parameter Estimation Using Line Correspondence

For the localization of the mobile robot, we are going to obtain ${}^{W}H_C = \begin{bmatrix} R & T \\ 0 & 1 \end{bmatrix}$ as well as the camera internal parameters, S and f, using the line correspondences (Lui et al., 1990; Luong and Faugeras, 1997).

Let us denote a straight line, J (refer to Figure 4) as

$$ \mathrm{J} : \mathrm{P_j} = \mathrm{n_w} t + \mathrm{P_i} \tag{9} $$

where $\mathrm{n_w}$ represents the directional vector of the straight line, t represents a constant, and $\mathrm{P_i}$ and $\mathrm{P_j}$ are positioning vectors for the point U and V *w.r.t.* the world frame, respectively.

A two dimensional line L can be represented as follows :

$$ \mathrm{L} : Ax_i + By_i + C = 0 \tag{10} $$

where A, B and C can be determined by a constraint equation, $A^2+B^2+C^2=1$ and two equations corresponding to the two points. Substituting equation (2) and (3) into equation (10), we obtain the following plane equation :

$$ \mathrm{M} : Ax_c + By_c + f^{-1}Cz_c = 0 \tag{11} $$

The vector N is defined as a normal to the projecting plane M,

$$ \mathrm{N} = [A \quad B \quad f^{-1}C]^T \tag{12} $$

Note that this normal vector N is always orthogonal to the three dimensional line J. The directional vector for the 3-D line J can be denoted as $\mathrm{n_c}$ and represented in terms of the camera frame as

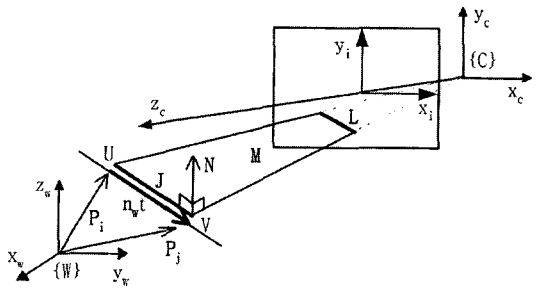

Fig. 4 Projecting plane of a 3-D line and a 2-D line

$$n_c = R^T n_w \tag{13}$$

Since the 3-D line J is located on the projecting plane, M, and the directional vector of J is orthogonal to the normal vector of the projecting plane, we have

$$n_c \cdot N = 0 \tag{14}$$

This represents the main idea for obtaining the camera parameters. Substituting equation (13) into (14), and using the fact that inner product of two orthogonal vectors can be represented as a product of two vectors, we have

$$n_w{}^T R N = 0 \tag{15}$$

Let us consider two points in 3-D space, U and V, and the corresponding two points in the image plane, $P_i(X_i, Y_i)$ and $P_j(X_j, Y_j)$. Plugging P_i and P_j coordinates into equation (10), and solving the two equations for the line coefficients, A, B and C, we have

$$A = (Y_j - Y_i) \tag{16a}$$

$$B = (X_j - X_i) \tag{16b}$$

$$C = (X_j Y_i - X_i Y_j) \tag{16c}$$

Since the directional vector, n_w, of the 3-D line is parallel to the line passing through the two points, U and V, it can be denoted as

$$n_w = (P_i - P_j) / \| P_i - P_j \| \tag{17}$$

Utilizing $\bar{x}_i = S_x x_i$ in (4) to separate S from x_i, and substituting this into equation (16a) through (16c), the normal vector (12) is represented as

$$N = [A \quad S^{-1}B \quad S^{-1}f^{-1}C]^T \tag{18}$$

Now, let us describe the process of obtaining camera parameters using (15). Substituting (17) and (18) into (15), we have

$$[i \quad j \quad k] \begin{bmatrix} r_1 & r_2 & r_3 \\ r_4 & r_5 & r_6 \\ r_7 & r_8 & r_9 \end{bmatrix} \begin{bmatrix} A \\ S^{-2}B \\ S^{-1}f^{-1}C \end{bmatrix} = 0 \tag{19}$$

where the parameters A, B, and C are obtained by (16a) through (16c) and the directional vector $n_w = [i \ j \ k]^T$ is obtained by (17). Equation (19) can be changed to equation (20) by decomposing known variables and unknown variables as follows:

$$[iA \ iB \ iC \ jA \ jC \ kA \ kB \ kC] \begin{bmatrix} S \cdot r_1 \cdot r_5^{-1} \\ r_2 \cdot r_5^{-1} \\ f^{-1} \cdot r_3 \cdot r_5^{-1} \\ S \cdot r_4 \cdot r_5^{-1} \\ f^{-1} \cdot r_6 \cdot r_5^{-1} \\ S \cdot r_7 \cdot r_5^{-1} \\ r_8 \cdot r_5^{-1} \\ f^{-1} \cdot r_8 \cdot r_5^{-1} \end{bmatrix} = -jB \tag{20}$$

Note that even though there are nine variables $r_1 \cdots r_9$ in R, only three of them are independent. Note also that the variables in the second vector of (20) are independent from the coordinates of the two points; depending upon the camera specifications and the rotation matrix. Therefore, if we obtain 8 equations of (20) corresponding to 8 lines in the image frame, a matrix equation can be obtained by superposing the equations, which can be represented as

$$M_{8\times 8} X_{8\times 1} = B_{8\times 1} \tag{21}$$

where $X_{8\times 1}$ is the second vector in (20). Now, the unknown camera parameters can be obtained by multiplying the inverse of M at both sides of (21). We have an over-determined system of (21) which can be solved by least squares method (Tsai, 1987). In practice, there may be several dependent rows in the matrix, $M_{8\times 8}$. Therefore, instead of multiplying inverse of $M_{8\times 8}$ directly, the matrix is decomposed by the singular value decomposition as $M_{8\times 8} = UDV^T$, and the matrix $X_{8\times 1}$ is obtained as follows:

$$X = V \cdot D^{-1} \cdot U^T \cdot B \tag{22}$$

where $D^{-1} = \begin{bmatrix} \Sigma^{-1} & 0 \\ 0 & 0 \end{bmatrix}$, $\Sigma = diag[\sigma_1, \ \sigma \cdots \sigma_m]$, σ_1 to σ_m represent the positive singular values of M, and $D \in R^{8\times 8}$ and $V \in R^{8\times 8}$ are left and right eigenvector matrices.

Notice that this active calibration scheme provides the line segments consecutively so that the rank of M can be increased to five by adding or replacing rows obtained by new line segments at any cases. Calibration of the individual parameters from X is straight-forward (Han and Lee, 1997).

Now, the correspondences of the feature points are used to calculate the translational vector T of the camera frame. By changing (1) as (23), and substituting this equation into (2) and (3), we have the coordinates of the feature point on the image frame as (24) and (25):

$$p_c = R^{-1}p_w - R^{-1}T = p'_w - T' \tag{23}$$

$$x_i = f\frac{x'_w - T'_x}{z'_w - T'_z} \tag{24}$$

$$y_i = f\frac{y'_w - T'_y}{z'_w - T'_z} \tag{25}$$

where $p'_w = (x'_w, y'_w, z'_w)^T$ and T' represent a positioning vector and a translation vector in terms of the camera frame, respectively. To obtain the translation vector T' from (24) and (25), the following matrix equation is derived:

$$\begin{bmatrix} f & 0 & -x_i \\ 0 & f & -y_i \end{bmatrix}\begin{bmatrix} T'_x \\ T'_y \\ T'_z \end{bmatrix} = \begin{bmatrix} f\cdot x'_r - x_i\cdot z'_r \\ f\cdot y'_r - y_i\cdot z'_r \end{bmatrix} \tag{26}$$

For a given feature point, (x_r, z_r), the matrix equation (26) provides two linear equations. Therefore, if we have two feature points, four linear equations are obtained for the three unknowns, T'_x, T'_y and, T'_z.

Now, the homogeneous transformation from the world frame to the camera frame, ${}^{W}H_C$ is completely obtained by (20) and (26). Substituting ${}^{W}H_C$, into (6), we can calculate ${}^{W}H_B$ which represents the position/orientation of the end plate of the mobile robot.

5. Active Calibration Using Conic Correspondence

To use the line correspondence scheme for the active calibration, there should be straight line segments in an object. However, for a cylindrical object, they are not available. In this section, an active calibration scheme for the circular shapes is introduced, which is applicable to the cylindrical or conic objects. Two sequential images captured by a CCD camera are used to obtain a conic parameter matrix and to complete the calibration algorithm.

From the two circular images, we extract two ellipsoids and estimates conic parameters. After the two conic parameters are obtained, the active calibration process is followed to get the rotation matrix, R, and finally the translational vector, T'.

5.1 Conic parameter estimation

Many man-made objects have circles on their surface. Researchers have presented several methods of estimating conic parameters from given data points (Davies, 1989; Zhang, 1997). Typical methods to solve the curve fitting problem are the least square, Hough transform, and area moments methods (Safaee-Rad et al., 1991; Maybank and Faugeras, 1992). Among these methods, the least square method is popular because of its computational efficiency. In this paper we apply the least square method for the curve fitting algorithm to obtain the conic parameter matrix.

Let us consider the second order equation (27) defining the conics in a plane. In an image plane, a second-order conic equation is represented as

$$aX^2 + bXY + cY^2 + dX + eY + f = 0 \tag{27}$$

where a, b, c, d, e, and f are conic parameters that determine the shape of the second order equation.

Equation (27) is re-formulated with a general vector $u = [X \;\; Y \;\; 1]^T$ and a coefficient matrix, A as follow:

$$u^T A u = 0 \tag{28}$$

where the A matrix is defined as a symmetric conic coefficient matrix, that is,

$$A = \begin{bmatrix} a & b/2 & d/2 \\ b/2 & c & e/2 \\ d/2 & e/2 & f \end{bmatrix} \tag{29}$$

In order to estimate the conic coefficient matrix A, we need to get the image coordinates, (x_i, y_i)'s, on the conic. The coordinates are obtained from the image captured by a CCD camera through the image processing. There may exist some error in capturing and processing the image. To reduce the error, the conic coefficients are adjusted by fitting the image coordinates to the

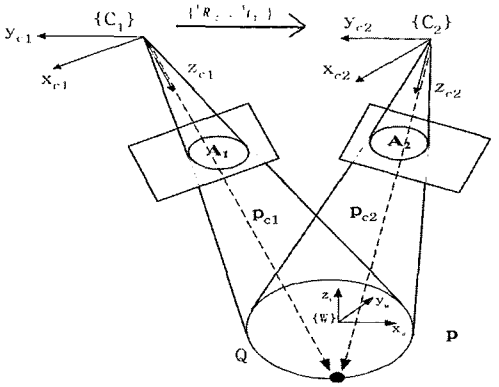

Fig. 5 Geometric structure for capturing conic images

curve equation. The least-square error criterion is used to fit a conic equation to the coordinates of N points on a conic image.

5.2 Active calibration using conic object

If we use a camera for the active calibration, multiple images need to be captured at different postures of the camera. That is, two different images captured by a camera are utilized for the active calibration. Figure 5 displays the geometric structure of the camera capturing two images at the different postures. The relationship between two cameras coordinate system is represented as

$$p_{c1}={}^1R_2 p_{c2}+{}^1t_2 \tag{30}$$

where ${}^1R_2$ represents a rotation matrix from $\{C_1\}$ to $\{C_2\}$ and ${}^1t_2$ is a translation vector from $\{C_1\}$ to $\{C_2\}$.

5.2.1 Geometric properties of a conic and its image

The representative of a second order equation is a conic. In this section, we restrict shapes of images to circles and ellipsoids. In Figure 5, suppose a conic in a space lies on a plane, p, and a world frame, {W}, is defined on the plane p such that x_w and y_w axes lie on this plane and z_w axis is normal to the plane p.

The camera coordinate systems $\{C_1\}$, $\{C_2\}$, and the world frame {W} are related as

$$p_w={}^iR_0 p_w+{}^it_0,\ i=1,\ 2 \tag{31}$$

where ${}^iR_0$ and ${}^it_0$ represent a rotation matrix and a translation vector from the world frame to the i-*th* camera frame, $p_{ci}\equiv[x_{ci}\ y_{ci}\ z_{ci}]^T$, and $p_w\equiv[x_w\ y_w\ z_w]^T$.

Any point on the plane, p, can be represented *w.r.t.* $\{C_1\}$ and $\{C_2\}$ as follows:

$$p_{ci}=G_i u_w,\qquad i=1,\ 2 \tag{32}$$

where G_i is a matrix defined as $G_i\equiv[{}^ir_1\ {}^ir_2\ {}^it_0]$, ${}^ir_1$ and ${}^ir_2$ are the first and second column vectors of ${}^iR_0$, respectively, and $u_w(=[x_w\ y_w\ 1]^T)$ represents a point on the plane, p, *w.r.t.* the world frame.

Equation (32) represents the relation between the world coordinates and the camera coordinates. Using equations (2) and (3), equation (32) yields

$$z_{ci}u_i=G_i u_w,\qquad i=1,\ 2 \tag{33}$$

where $z_{ci}(=z_c/f)$ becomes a scaling factor for G_i and $u_i=[x_i\ y_i\ 1]^T$.

Suppose a conic in the plane is represented by

$$u_w^T Q u_w=0,\qquad i=1,\ 2 \tag{34}$$

then we can obtain the shape of the curve by analyzing the elements of the matrix Q. Let us assume that we have two conics in the image plane represented as

$$u_i^T A u_i=0,\qquad i=1,\ 2 \tag{35}$$

The conic parameter matrices, A_1 and A_2, can be obtained by the curve fitting algorithm with the conic images. Plugging equation (33) into equation (35) assuming the scale factor, $z_{ci}=1$; we have

$$u_w^T G_i^T A_i G_i u_w=0,\qquad i=1,\ 2 \tag{36}$$

Since the conics in (36) and (34) have the same shape,

$$G_i^T A_i G_i=k_i Q,\qquad i=1,\ 2 \tag{37}$$

From the above equations, G_i can be obtained using the known A_i and Q. Note that since $G_i\equiv[{}^ir_1\ {}^ir_2\ {}^it_0]$, we can obtain ${}^iR_0$ and ${}^it_0$ from G_i, directly.

5.2.2 Conic-based correspondence

Two sequential images of a conic Q representing a real object are extracted and symbolized

by matrices A_1 and A_2 with the aid of a curve fitting algorithm. The relationship between a real object and two images are expressed as follows:

$$G_1^T A_1 G_1 = k_1 Q \tag{38}$$

$$G_2^T A_2 G_2 = k_2 Q \tag{39}$$

where $G_1=[{}^1r_1 \ {}^1r_2 \ {}^1t_0]$, $G_2=[{}^2r_1 \ {}^2r_2 \ {}^2t_0]\cdot[{}^1r_1 \ {}^1r_2]$, and $[{}^2r_1 \ {}^2r_2]$ are first two columns of ${}^1R_0$ and ${}^1R_1$, respectively.

As it is shown in Figure 5, the relationship between the two camera coordinate systems can be represented as

$${}^0R_2 = {}^0R_1 {}^1R_2 \tag{40}$$

$${}^0t_2 = {}^0R_1 {}^1t_2 + {}^0t_1 \tag{41}$$

Note that the homogeneous transformation between $\{C_1\}$ and $\{C_2\}$, that is, ${}^1R_2$ and ${}^1t_2$ are known a priori, since the robot carries the camera from $\{C_1\}$ to $\{C_2\}$ under the control.

The conic Q in the system $\{W\}$ is represented as

$$Q=\begin{bmatrix} q_{11} & 0 & q_{13} \\ 0 & q_{22} & 0 \\ q_{31} & 0 & q_{33} \end{bmatrix} \tag{42}$$

where $q_{11}=1/a^2$, $q_{22}=1/b^2$, $q_{13}=q_{31}=0$, and $q_{33}=-1$ when the conic Q is an ellipsoid.

There are six unknown parameters in ${}^iR_0$ and ${}^it_0$. Therefore, we have sixteen unknown parameters in total including k_1, k_2, q_{11}, and q_{22} in the equations (38) and (39). In general, these sixteen parameters can be generally solved by using the eighteen equations of (38), (39), (40), and (41).

Now we introduce a schematic approach to solve for the rotation matrix ${}^0R_i$, independently. From equations (38) and (39), we have

$$({}^1R_0^T A_1 {}^1R_0)^{2\times 2} = k_1 (Q)^{2\times 2} \tag{43}$$

$$({}^2R_0^T A_2 {}^2R_0)^{2\times 2} = k_2 (Q)^{2\times 2} \tag{44}$$

where $(X)^{2\times 2}$ represents the 2×2 upper-left sub-matrix of X.

From equations (43) and (44), we obtain

$$({}^1R_0^T A_1 {}^1R_0 - k^2 {}^1R_0^T A_2 {}^2R_0)^{2\times 2} = \begin{bmatrix} 0 & 0 \\ 0 & 0 \end{bmatrix} \tag{45}$$

where $k=k_1/k_2$ and ${}^0R_2={}^0R_1{}^1R_2$.

Note that ${}^1R_2$ is known a priori by the joint angles of the robot. Therefore, there are only four unknown parameters in the four equations provided by (45). Therefore, the rotation matrix ${}^1R_0$ can be determined uniquely. Plugging the obtained ${}^1R_0$ into equation (43) provides the solution for the k_1, q_{11}, and q_{22}.

Now to obtain the translation vector, ${}^1t_0$, let us use the facts that $q_{31}=0$, $q_{32}=0$ from equation (38). Then we have

$${}^1t_0^T A_1 {}^1r_1 = 0 \tag{46}$$

$${}^1t_0^T A_1 {}^1r_2 = 0 \tag{47}$$

$${}^2t_0^T A_2 {}^2r_1 = 0 \tag{48}$$

where ${}^2t_0$ can be replaced by terms of ${}^1t_0$ by equation (41). Therefore, we can have a unique solution for ${}^1t_0$ using the three linear equations.

Consequently, we can obtain the position and orientation parameters of camera, ${}^1t_0$ and ${}^1R_0$ from the two ellipsoid images captured by a camera at the task robot.

6. Experiments

6.1 Results of active calibration using line-correspondence

Assembly operations of hexagonal bolts and nuts are considered as an experimental environment. A CCD camera, SFA-410ED, that captures 60 image frames per second and each image frame has 768×494 pixels and the image area of 6.54 mm$\times$4.89 mm, is selected for our experiments. The values of dx and dy are calculated directly, and they are 0.0085 mm and 0.0098 mm, respectively. The standard focal length of the lens for this camera is 16 mm.

We placed a bolt on a table and the vertices of the bolt head are used for the feature points, whose coordinates are (0, 4, 0.42), (−4, 3, 0.42), (−5, −2, 0.32), (−1, −4, 0.4), (3, −3, 0.4), and (4, 2, 0.25) *w.r.t.* the world frame. To estimate the camera parameters, the orientation and position of the camera frame is initially matched to the world frame. And then, the camera frame is translated by [0, −18, 33.6] cm and rotated

150° along the x-axis. The image of bolt head is captured by the camera at frame $\{C_1\}$. For the extraction of vertices, we used the instructions given by the image processing board. First, we extracted the line edge in the preprocessing stage, and we used Hough transform for the detection of a line, which is robust against noises in the image. After obtaining six Hough transformation equations of lines, we extracted vertex-points solving the line equations.

Table 1 shows the sample data for the measurement of the focal distance, f, scale factor, S, Z-Y-Z Euler angles and the translational vector, T.

Table 2 shows the estimated values of the camera pose with the real values. The rotation is given along the y-axis only. Figure 6 represents the real images of hexagonal shapes used in experiment of table 2. The error represents the % magnitude error of the estimated translation vector compared to the real translation vector. As it is shown in table 2, the % error is small enough to compensate the real positioning error of a mobile robot. The rotation angle is estimated very precisely with negligible amount of error. Therefore, we claim that this scheme is applicable for the calibration of a mobile robot and also for the estimation of the position/orientation of the base of a task robot.

Figure 7 represents relative errors in the rotation and moving distance of camera with respect to the % of pixels affected by the noise. Through this experiment, the effects of noises occurring from image processing and illumination are analyzed. For the experiment, the noises are directly added to the pixels of the hexagonal object image: the camera parameter, f, is 17.5 mm; the position is (0, 20.6, 30.4) cm; the orientation is (144.4^0, 0^0, 0^0) in Z-Y-Z Euler angles. The noise has the normal distribution of the mean, 0 and the variance, 1. As it is shown in Fig. 7, the relative rotation error is less than 0.5° o and the relative position error is less than 0.3 mm until 15% of pixels are polluted by the noises, which are small enough to be ignored for the nominal task executions.

Table 1 Estimation of camera parameters

f(mm)	S	Translation vector T		Euler angle (°)	
17.542	0.9969	T_x	−0.1567	α	149.5
		T_y	−17.9703	β	3.4
		T_z	33.6506	γ	0.0

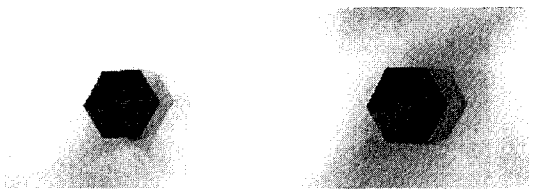

(a) Rotation angle, 160° (b) Rotation angle, 155°

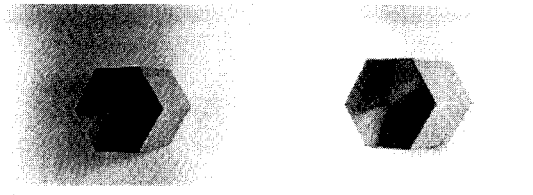

(c) Rotation angle, 150° (d) Rotation angle, 145°

Fig. 6 Images of hexagonal shapes rotated along the y_c axis

Table 2 Estimated values for hexagonal objects

Angle (°)	Real value(cm), (x, y, z)	Estimated value(cm), (x, y, z)	Error (%)
160	10.5, 0.1, 34.2	10.390, 0.099, 33.841	1.05
155	11.7, 0.1, 30.3	11.524, 0.098, 29.845	1.50
150	13.3, 0.1, 26.6	13.524, 0.196, 26.055	2.05
145	14.1, 0.1, 23.5	13.691, 0.097, 22.819	2.90
Average			1.88

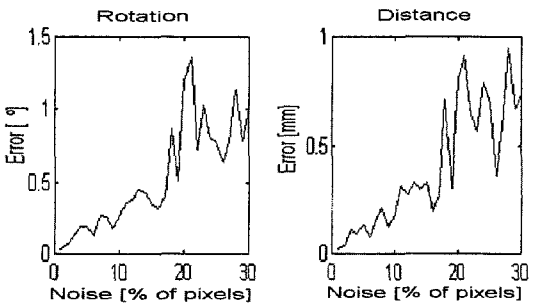

(a) Relative rotation (b) Relative position

Fig. 7 Relative errors of camera pose with additional noise

6.2 Results of active calibration using conic-correspondence

We also carried out experiments estimating the camera pose using the relationship between a conic in the three dimensional space and conics in the image plane. The camera and image processing system in this experiment is same as that of Section VI-A. The diameter of the cylinder is 40 mm and the center coordinates of the conic are set to the origin of world frame.

Two images of the cylinder are captured by a CCD camera for the active calibration. Table 3 shows the estimated position of camera with respect to the cylinder according to the rotation of the camera along the y_c axis. The first image is captured after aligning the center of image to the center of camera ; the second image is captured after rotating the camera along the y_c axis and translating along the x_c axis with the amount shown in table 3. Figure 8 shows the real images of a cylinder used in the experiment.

Table 3 Estimated position values and % error of camera for a cylinder

Angle (°)	Real value(cm), (x, y, z)	Estimated value(cm), (x, y, z)	Error (%)
160	18.19, 0.2, 50	17.981, 0.197, 49.150	1.63
155	23.31, 0.1, 50	23.009, 0.099, 49.375	1.17
150	28.86, 0.1, 50	28.611, 0.099, 49.500	1.04
145	35.01, 0.1, 50	34.667, 0.099, 49.525	0.97
Average			1.19

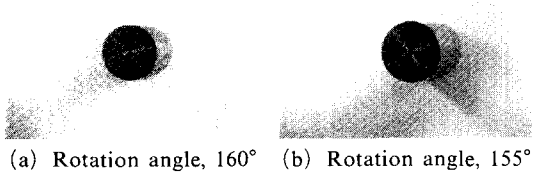

(a) Rotation angle, 160° (b) Rotation angle, 155°

(c) Rotation angle, 150° (d) Rotation angle, 145°

Fig. 8 Images of cylinder rotated along the axis

The edge data of conics are used to obtain the conic coefficient matrix through the curve fitting algorithm. There is an exceptional case that the camera rotates along the optical axis, z_c axis. In this case, the features of conics projected onto the image plane are the same in the two different frames, so the conic coefficients become underdetermined.

As shown in the experimental results, the conic correspondence provides more accurate data than the line correspondence in the active calibration.

In Figure 9, a red pyramid represents the position and orientation of each camera. The extrinsic parameters (relative positions of the object with respect to the camera) are then shown in a form

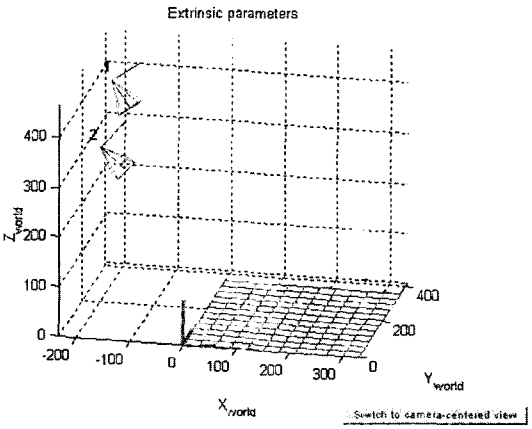

(a)

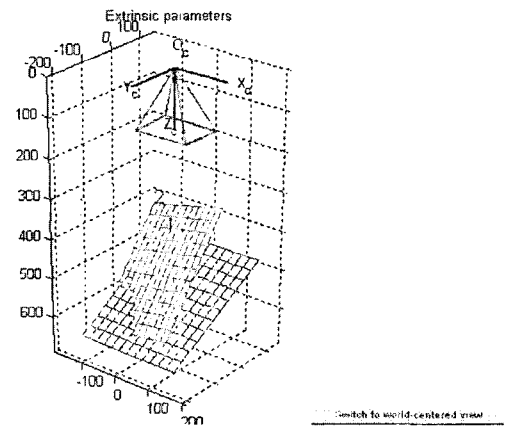

(b)

Fig. 9 Position/Orientation of robot end-effector with respect to a world frame

of a 3-D plot for the experimental results using conic correspondence. In this figure, the frame (O_C, X_C, Y_C, Z_C) is the camera reference frame. The red pyramid corresponds to the effective field of view of the camera defined by the image plane.

7. Conclusions

A new active calibration scheme is developed to estimate the position/orientation of a mobile robot working in the various environments. The main difficulty residing in the precise control of a mobile/task robot is providing an accurate and stable base for the task robot. In this research, the position of mobile robot is obtained by the active calibration scheme using the images captured by a camera at the hand of the task robot. In other words, the correspondence of the image coordinates to the real object coordinates is the basis for this scheme. This scheme is applied to the work-pieces of both the polygonal and the cylindrical.

For a polygonal object composed of points or lines, while the task robot is approaching to the object, the position of the camera is estimated using the line correspondence between the lines on the image captured by the camera and the lines of the real object. For the cylindrical or ball-shaped objects, there are not enough line segments for the calibration based on the line correspondence. For these objects, the conic-correspondence scheme is developed. That is, two conic parameter matrices that can be obtained from the two consecutive elliptic images and a homogeneous transformation matrix are used for obtaining the position and orientation of the camera. Note that the homogeneous transformation matrix that defines the relationship between the two frames where the images are captured can be calculated by using the joint angles of the robot.

Our future research topics are reducing the estimation errors and capturing two successive frames effectively adapting the environmental variations.

References

Aloimonos, J., Weiss, I. and Bandyopadhyay, A., 1988, "Active Vision," *Int. Journal of Computer Vision*, Vol. 1, No. 4, pp. 333~356.

Davies, E. R., 1989, "Finding Ellipses Using the Generalized Hough Transform," *Pattern Recognition Letters*, Vol. 9, pp. 87~96.

Du, F. and Michael Brady, 1993, "Self-Calibration of the Intrinsic Parameters of Cameras for Active Vision Systems," Proc. IEEE. Conf. on Computer Vision and Pattern Recognition, pp. 15~17.

Han, M. Y. and Jang M. Lee, 1997, "Precision Control of a Mobile/Task Robot Using Visual Information," *Journal of The Korea Institute of Telematics and Electronics, in Korea*, Vol. 34, No. 10, pp. 1089~1097.

Hanqi Zhuang and Zvi S. Roth, 1996, Camera-Aided Robot Calibration, CRC Press.

Heyden, A. and Astrom, K., 1997 "Euclidean Reconstruction from Image Sequences with Varying and Unknown Focal Length and Principal Point," Proc. IEEE Int. Conf. on Computer Vision and Pattern Recognition, pp. 438~443.

James L. Crowley and Philippe Bobet, 1993, "Dynamic Calibration of an Active Stereo Head," *International Journal of Computer Vision*, pp. 734~739.

Jin-Gu Kang, Tae-Seok Jin, Min-Gyu Kim and Jang-Myung Lee, 2000, "Optimal Configuration Control for a Mobile Manipulator," *KSME International Journal*, Vol. 14, No. 6, pp. 605~621.

Jin-Hee Jang and Chang-Soo Han, 1997, "The State Sensitivity Analysis of the Front Wheel Steering Vehicle : In the Time Domain," *KSME International Journal*, Vol. 11, No. 6, pp. 595~604.

Johann Borenstein, 1995, "Control and Kinematic Design of Multi-Degree-of-Freedom Mobile Robots with Compliant Linkage," IEEE Trans. on Robotics and Automation, Vol. 11, No. 1, pp. 21~35.

Longuet-Higgins, H., C., 1981, "A Computer Algorithm for Reconstructing a Scene from two

Projections," in Nature, Vol. 293, pp. 133~135.

Luong, Q. T. and Faugeras, O. D., 1997, "Self-Calibration of a Moving Camera from Point Correspondences and Fundamental Matrices," International Journal of Computer Vision, Vol. 22, No. 3, pp. 261~289.

Pollefeys, M., Koch, R. and Gool, L. Van, 1998, "Self-Calibration and Metric Reconstruction in Spite of Varying and Unknown Internal Camera Parameters," In International Conference on Computer Vision, pp. 90~95.

Radu Horaud, Fadi Dornaika, Bart Lamiroy, and Stephane Christy, 1997, "Object Pose : The Link between Weak Perspective, Paraperspective, and Full Perspective," *International Journal of Computer Vision*, Vol. 22, No. 2, pp. 173~189.

Roger Pissard-Gibollet and Patrick Rives, 1995, "Applying Visual Servoing Techniques to Control a Mobile Hand-Eye System," Proc. IEEE Int. Conf. on Robotics and Automation, Nagoya, Japan, pp. 166~171.

Safaee-Rad, R. Rchoukanov, I. Benhabib, B. and Smith, K. C., 1991, "Accurate Parameter Estimation of Quadratic Curves from Grey-Level Images," Comput. Vis. Graph. Image Process.: Image Understanding, Vol. 54, No. 2, pp. 259~274.

Stephen J. Maybank and Olivier D. Faugeras, 1992, "A Theory of Self-Calibration of a Moving Camera," *International Journal of Computer Vision*, Vol. 8, No. 2, pp. 123~151.

Sturm, P. and Maybank, S., 1999, "On Plane-Based Camera Calibration : A General Algorithm, Singularities, Applications," Proc. IEEE Int. Conf. on Computer Vision and Pattern Recognition, Fort Collins, USA, pp. 432~437.

Tsai, R. Y., 1987, "A Versatile Camera Calibration Technique for High Accuracy 3-D Machine Vision Metrology Using o_-the-Shelf TV Cameras Lenses," IEEE Trans. on Robotics and Automation, Vol. 3, pp. 323~344.

Yi Ma, Jana Kosecka and Shankar Sastry, 1999, "Optimization Criteria and Geometric Algorithms for Motion and Structure Estimation," UC Berkeley Memorandom, No. UCB/ERL M99/33, p. 35.

Yuncai Lui, Thomas S. Huang, and Olivier D. Faugeras, 1990, "Determination of Camera Location from 2-D to 3-D Line and Point Correspondences," IEEE Trans. on Pattern Analysis and Machine Intelligence, Vol. 12, No. 1, pp. 28~37.

Zhengyou Zhang, 1997, "Parameter Estimation Techniques : A Tutorial with Application to Conic Fitting," Image and Vision Computing, Vol. 15, No. 1, pp. 57~76.

Zhuang, H., Roth, Z. S. and Wang, K., 1991, "Robot Calibration by Mobile Camera System," in Proc. ASME Winter Ann. Mtg. Invited Session on Image Process. Appl. Process Automation, DSC-Vol. 30, pp. 62~65.